Simulations of Solar Radiative Transfer in Measured and Generated Cloud Fields

Sebastián Gimeno García and Thomas Trautmann

Zusammenfassung

Um ein besseres Verständnis des Einflusses von Wolken auf den Strahlungstransport zu erlangen, müssen neben direkten Messungen der Strahlungsgrößen auch Strahlungstransportrechnungen durchgeführt werden. Dabei werden mikrophysikalische Eigenschaften aus Fernerkundungs- und in situ Messungen sowie generierte Wolkenfelder verwendet.

In den BBC1- und BBC2 (= **B**altex **B**ridge **C**loud 1 und 2)-Messkampagnen wurden Messungen der mikrophysikalischen Wolkeneigenschaften und der Strahlungsgrößen durchgeführt. In diesem Bericht werden Ergebnisse von spektralen Monte Carlo Simulationen des Strahlungstransports in der Kurzwellenregion für Wellenlängen zwischen 350 nm und 850 nm für einen in BBC1 gemessenen Stratocumulus gezeigt. Zusätzlich wurden auch Strahlungstransportssimulationen für einen LES (= **L**arge **E**ddy **S**imulation)-simulierten Cumulus und für eine entsprechende IAAFT (= **I**terative **A**mplitude **A**dapted **F**ourier **T**ransform)-Surrogatwolke mit denselben statistischen Eigenschaften wie die ursprüngliche Wolke durchgeführt.

Summary

For a better understanding of the role that clouds play in the radiative transfer (RT) across the atmosphere, computer RT simulations with microphysical data retrieved from remote sensing and in situ measurements as well as with cloud fields provided by cloud generators have to be carried out in addition to field measurements campaigns.

In this work we show spectral RT results for two cloud studies. During the BBC1 and BBC2 (=**B**altex **B**ridge **C**loud 1 and 2) campaigns measurements of cloud radiation and microphysics properties have been performed. We present here the results of a series of quasi-spectral simulations covering the shortwave region (from 350 nm up to 850 nm) for a remote-sensing captured stratocumulus. RT calculations have also been carried out for a LES (=**L**arge **E**ddy **S**imulation) cumulus and an IAAFT (=**I**terative **A**mplitude **A**dapted **F**ourier **T**ransform) surrogate cloud with the same statistics as the original.

1 Introduction

The Earth's radiation budget is strongly influenced by clouds as they reflect solar radiation and absorb terrestrial thermal radiation. Clouds modulate the radiative driving of the climate models, causing large uncertainties in the determination of climate sensitivity to either natural or anthropogenic changes. Furthermore, clouds are the main heterogeneous part of the atmosphere and therefore dominate our perception of the weather. Even though, the parameterization of clouds in both, climate and numerical weather prediction models is still completely inappropriate.

The 4DCLOUDS project (4DCLOUDS (2004)) was conceived to capture the radiative influence of inhomogeneous clouds and to implement these influences in the modeling of transport and exchange processes in dynamical atmospheric models. To carry out

this challenging task it is necessary to investigate the issue both, experimentally and theoretically.

The experimental part of the 4DCLOUDS project was executed in two measurement campaigns. The first one, the Baltex Bridge Cloud (BBC1) campaign (BBC1 (2004)), was organized together with the EU-project CLIWA-NET (=**C**oud **LI**quid **WA**ter **NET**work) (CLIWA-NET (2004)) and was carried out in The Netherlands around Cabauw in August and September 2001. The second measurement campaign, the Baltex Bridge Cloud 2 (BBC2) (BBC2, 2004), was organized by the University of Bonn (project coordinator of the 4DCLOUDS project) and KNMI (=**K**oninklijk **N**ederlands **M**eteorologisch **I**nstituut (KNMI, 2004)) (coordinator of the Cabauw measurement site and member of CESAR (=**C**abauw **E**xperimental **S**ite **A**tmospheric **R**esearch) (CESAR (2004))) and took place in May 2003 also around Cabauw.

On the other hand multi-dimensional high-spectral-resolved radiative transfer (RT) simulations are being performed. In order to be able to make realistic realizations, RT models require information on cloud morphology and on the microphysics of aerosol particles and cloud drops. This input data can be obtained from the combination of in situ measurements and dedicated ground-based and satellite observations. Other possibilities to get this input data are to use cloud-resolving dynamical models, such as GESIMA (=**Ge**esthacht **Si**mulation **M**odel of the **A**tmosphere) (GESIMA (2004)), the LM (=**L**okal-**M**odell) of the German Weather Service (LM (2004)) and LES (=**L**arge **E**ddy **S**imulation) models (e.g. Deardorff (1972)) or by using fractal cloud generators (e.g. (Venema *et al.*, 2003)). Additionally, one-dimensional (1D) RT calculations by means of the perturbation theory are carried out in order to derive an improved parameterization of the radiative properties of the cloudy atmosphere.

In this work we present results (Section 5) of RT realizations by means of the Monte Carlo (MC) method (Section 2) for two cloud scenarios: *i)* a cloud field measured on September 23rd, 2001 of the BBC1 campaign (Section 3) and *ii)* a three-dimensional (3D) LES-generated cloud field and one statistically generated surrogate of this particular cloud field (Section 4).

2 Radiative Transfer Model

The RT simulations are performed by means of the LMCM (=**L**eipzig **M**onte **C**arlo **M**odel). The LMCM uses the MC method to explicitly deal with the radiative processes that take place within the atmosphere. The LMCM yields downward and upward flux densities at all atmospheric levels, absorbed power in all atmospheric cells, net horizontal flux density between one cell and its neighbors, and actinic flux. For more detailed information see Gimeno and Trautmann (2003).

2.1 Atmospheric setup

The model atmosphere consists of a horizontally homogeneous background of ozone and oxygen —as the only major absorbing gases— and air molecules causing Rayleigh scattering. Cloud water content is the only component that varies in the horizontal. The HITRAN database (Rothman *et al.* (1998)) for specifying the spectral absorption characteristics of the atmospheric trace gases together with a midlatitude-summer standard profile (McClatchey *et al.* (1972)) are employed to derive absorption and scattering coefficients at different atmospheric levels ranging between 0 and 70 km. The spectral ground

albedo measured from the aircraft Partenavia (Wendisch *et al.* (2003)) in the BBC1 campaign is chosen (see Fig. 1). This spectral ground albedo was measured on the cloudless day of September 28th, 2001 of the BBC1 campaign. For all the 3D-RT calculations, periodic boundary conditions are assumed.

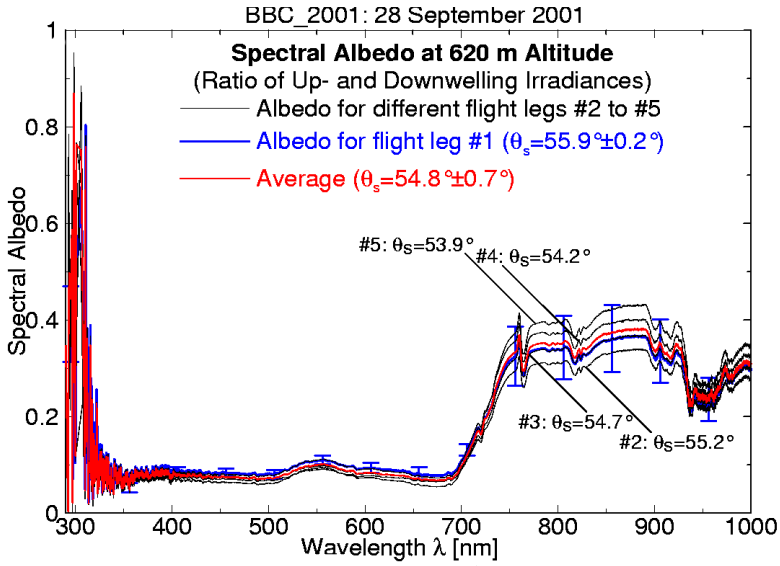

Figure 1: Airborne measurements of the ground albedo at an altitude of 620 m on the cloudless day of September 28th, 2001 of the BBC1 campaign. (M. Wendisch, personal communication)

2.2 Cloud optical properties

Cloud drop size distribution can be modelled by a three-parameter log-normal distribution:

$$n\left(r\right) = \frac{N_c}{\sigma\sqrt{2\pi}r}\,\exp\left[-\left(ln\,r - ln\,r_0\right)^2/2\sigma^2\right]\,, \tag{1}$$

where N_c is the total drop concentration, r_0 is the modal radius and σ is the logarithmic width of the distribution. The number of droplets within a unit volume from radii r to $r + dr$ is given by $n\left(r\right)dr$. The moments of the distribution are given by:

$$\left\langle r^k \right\rangle = \frac{1}{N}\int_0^\infty r^k n\left(r\right)dr = r_0^k \exp\left[k^2\sigma^2/2\right]\,. \tag{2}$$

The effective radius (r_{eff}) of the drop size distribution is defined as the ratio of the third moment to the second moment,

$$r_{eff} = \left\langle r^3 \right\rangle / \left\langle r^2 \right\rangle\,. \tag{3}$$

The liquid water content (LWC), i.e. the mass of liquid water per unit of volume, can be expressed as a function of the third moment as follows:

$$LWC = \left(4\pi/3\right)\rho_w N_c \left\langle r^3 \right\rangle = \left(4\pi/3\right)\rho_w N_c r_0^3 \exp\left(9\sigma^2/2\right)\,, \tag{4}$$

where ρ_w is the mass density of water.

The optical properties —in shortwave spectral region (SWSR)— of a homogeneous cloud volume is described by three parameters, namely: the cloud extinction coefficient, $\beta_{ext} = \beta_{sca} + \beta_{abs}$ —where β_{sca} and β_{abs} are the cloud scattering and absorption coefficient, respectively—, the single scattering albedo, $\omega_0 = \beta_{sca}/\beta_{ext}$, and the scattering phase function, $p(\theta)$ —where θ is the scattering angle. If the one-parameter Henyey-Greenstein (HG) phase function (PF) is chosen, it is sufficient to specify the asymmetry factor, $g = \int_0^{2\pi} p(\theta) \cos\theta \, d\theta$, (HGPFs yield, for example, complete forward scattering for $g = 1$, isotropic scattering for $g = 0$ and backward scattering for $g = -1$).

By means of the parameterization derived by Slingo (1989), these three optical parameters (β_{ext}, ω_0 and g) can be obtained as functions of LWC and r_{eff} for 24 spectral bands in the SWSR ($\lambda \in [0.25, 4.00]\ \mu m$):

$$\begin{array}{rcl} \beta_{ext,i} & = & LWC \left(a_i + \frac{b_i}{r_{eff}} \right), \\ 1 - \omega_{0,i} & = & c_i + d_i \cdot r_{eff}, \\ g_i & = & e_i + f_i \cdot r_{eff}, \end{array} \tag{5}$$

where the subscript i refers to the different spectral bands and the coefficients a_i, b_i, c_i, d_i, e_i, f_i can be found in Slingo (1989).

Unfortunately, the combination of collocated radar and microwave measurements do not provide all the information about the drop size distribution. Then, assumptions on the size distribution parameters (N_c, r_{eff}, σ) must be made when estimating the cloud microphysical properties.

In the cloud fields presented in the following sections the LWC is retrieved from measurements or is provided by cloud generators whereas r_{eff} reminds unknown. Thus, in order to use the Slingo parameterization (Eq. 5), assumptions on the r_{eff} must be made.

In the case of the LWC field measured on September 23rd, 2001 of the BBC1 (Fig. 3), we assumed a constant r_{eff} of $10\,\mu m$ over the whole cloud field. This assumption is widely adopted when accepted radiative transfer codes, as e.g. DISORT (=**DIS**crete **O**rdinate **R**adiative **T**ransfer model (Stamnes *et al.*, 1988)), are employed to compute radiative properties of horizontally homogeneous clouds. However, according to in situ cloud microphysics measurements this approximation is far from reality and assuming a constant cloud droplet number concentration N_c rather than a constant r_{eff} would be more suitable. One can keep on using the Slingo parameterization (Eq. 5) calculating r_{eff} as a function of LWC and N_c making use of the proportionality of r_{eff} to the volume mean radius, r_v,

$$r_{eff} = \gamma \, r_v = \gamma \sqrt{\frac{3}{4\pi\rho_w} \frac{LWC}{N_c}}, \tag{6}$$

where γ is the proportionality factor, ρ_w is the water density and N_c is the cloud droplet number concentration. Peng and Lohmann (2003) found a linear relationship between γ and N_c by fitting all the available liquid water data from the campaigns RACE and FIRE.RACE:

$$\gamma = 1.18 + 0.00045\, N_c\,. \tag{7}$$

In the case of the generated LWC-fields presented in section 4, we assumed a constant drop number concentration N_c of $1000\,cm^{-3}$ over the whole cloud field and the optical properties were calculated by means of the Eqs. 5, 6 and 7.

3 Measured cloud fields

The central station of the measurement campaigns BBC1 and BBC2 placed at Cabauw (The Netherlands) offered a great variety of ground-based remote sensing and meteorological instruments. This inimitable situation enabled to develop a new algorithm for retrieving the cloud liquid water content (LWC): the so-called Integrated Profiling Technique (IPT) (Löhnert *et al.*, 2003).

Common LWC-retrieval methods (e.g. Frisch *et al.* (1998)) scale the radar reflectivities to the liquid water path (LWP) derived from a microwave radiometer. The IPT applies the optimal estimation theory combining the microwave brightness temperatures (TB) measured by the multi-channel microwave radiometer MICCY (Crewell *et al.*, 2001), the attenuation-corrected radar reflectivity (Z) profiles measured by the 95GHz cloud radar MIRACLE (MIRACLE (2004)), the lidar-ceilometer cloud base, ground-level measurements of temperature and humidity, the nearest operational radiosonde profile and a reference single column LWC calculated with a cloud-resolving model using explicit microphysics and initiated with the local radiosonde profile.

Both methods were applied to all suitable conditions during the BBC1 and BBC2 campaigns, namely to all situations of non-precipitating single-layer liquid-water clouds. From the ground-based remote sensing point of view, the day of September 23rd, 2001 was the best day of the BBC1.

On that day, a compact stratocumulus cloud was observed for about two hours with high vertical resolution (see Fig. 2). A cut in the retrieved time series from 8:30 until 10:00h containing this compact stratocumulus field is chosen in this work to make the RT studies.

The domain used consisted of 1420 grid points in the horizontal and 88 vertical levels. Horizontal resolution was calculated by multiplying the radar acquisition time t=5 s and the average wind velocity at cloud altitude w=5.7 m/s, leading to a resolution of 28.5 m. The radar vertical resolution, 37.5 m, was used from the surface up to the upper most cloud level (1320 m). A coarser resolution for the additional upper layers was taken, ranging from the 200 m just above the cloud to the 10 km at the highest model atmospheric layer.

4 Generated cloud fields

For sensitivity studies one needs special predefined cloud characteristics depending on the phenomena under investigation. These ideal cases are either not available from real measurements or they are not numerous enough to statistically provide significant results. Fortunately, the RT calculations must not be constrained to the use of only measured cloud fields as input, but they can also be fed with realistic cloud fields generated by cloud models.

Cloud generators can be classified into physical and statistical. The first type takes into account the microphysical and meteorological properties of an atmospheric volume and let it evolve according to the laws of dynamics and thermodynamics (Scheirer and Macke, 2001). Since realizations with a reasonably limited CPU-time consumption are required, the spatial resolution of such models —specially in the vertical dimension— is strongly limited. The second type of generators provides surrogate fields of an original cloud (template) conserving some specific statistics without dealing with the physics that is behind the cloud formation process at all.

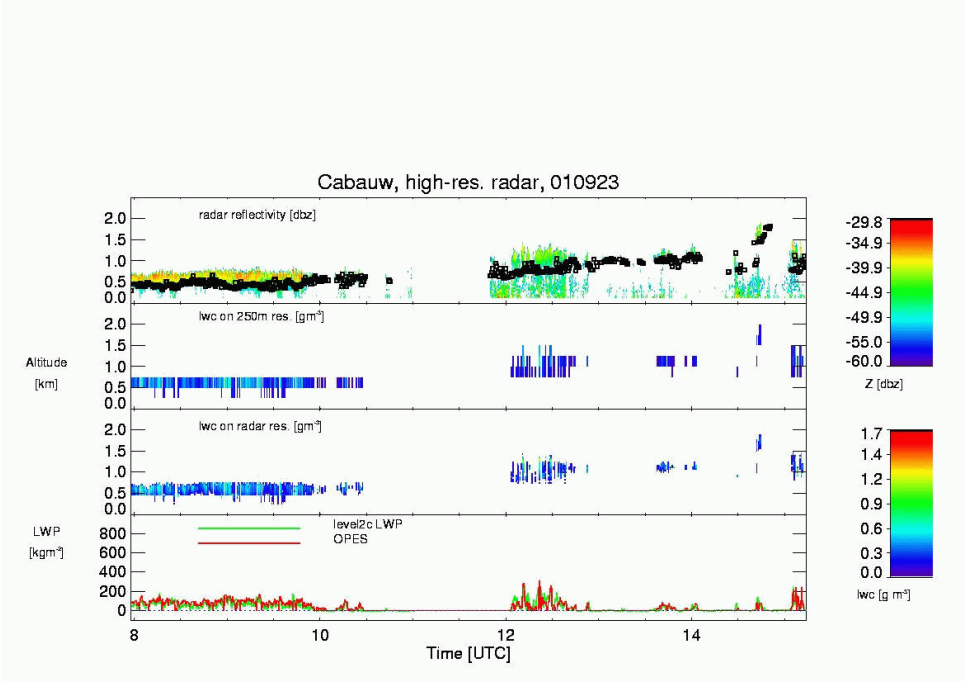

Figure 2: LWC field retrieved using the integrated profiling technique (IPT) for the day 09/23/01 of the BBC1 measurement campaign. From 8:30 until 10:00h the time series does not contain multi-layer clouds, precipitation, drizzle, ice clouds or mixed phases: a perfect scenario for applying the IPT. The plot at the top of the figure shows the radar reflectivities and the lidar cloud-base measurements (plotted as points). The two plots in the middle show the retrieved LWC on 250 m and 37.5 m vertical resolution. The plot at the bottom shows the LWP measured by the microwave radiometer MICCY (From U. Löhnert, BBC data bank)

Clouds show a fractal structure and this internal structure has an important impact on its radiative properties. Because of that a realistic LWC field is not satisfactorily described by means of one-point statistics, i.e. statistics related to the field as a whole (e.g. amplitude distribution), but also the use of two-point statistics is necessary, i.e. correlations between pairs of points at different scales (e.g. power spectrum).

Statistical generators are suitable when considering systematic sensitivity studies in which parameters such as the spatial organization can be changed and other quantities —such as cloud cover, total LWC and water variance— remain constant.

In this work we use a 3D-LES-simulated LWC field and one surrogate cloud that preserves its amplitude distribution and its power spectrum generated by means of the Iterative Amplitude Adapted Fourier Transform (IAAFT) Method (see Venema *et al.* (2003)) .

The domain used consisted of 66 x 66 grid points in the horizontal with a spatial resolution of 100 m and 69 vertical levels with varying resolution. Below the cloud, 4 layers with vertical resolution of 100 m were placed, within the cloud the distant between levels was set to 40 m and as in the previous case a coarser resolution for the additional upper layers was taken, from 1000 m just above the cloud to 5 km at the highest stratospheric layer.

5 Results

In this section the results of RT calculations obtained for the stratocumulus cloud measured on the day 09/23/01 of the BBC1 campaign as well as for a LES-simulated cumulus field and one IAAFT-surrogate are presented.

5.1 Radiative transfer for the day 09/23/01 of the BBC1 campaign

Making use of the Slingo parameterization (Eq. 5) with $r_{eff} = 10\mu m$ the LWC time series reconstructed from a composite of radar, microwave and lidar measurements via Frisch algorithm is transformed into the three 2D optical fields of $\beta_{ext}(x,z)$, $\omega_0(x,z)$ and $g(x,z)$. Figure 3 shows the 2D extinction coefficient field for the stratocumulus cloud captured on September 23rd of 2001 between 8:30 and 10:00h. Using the atmospheric

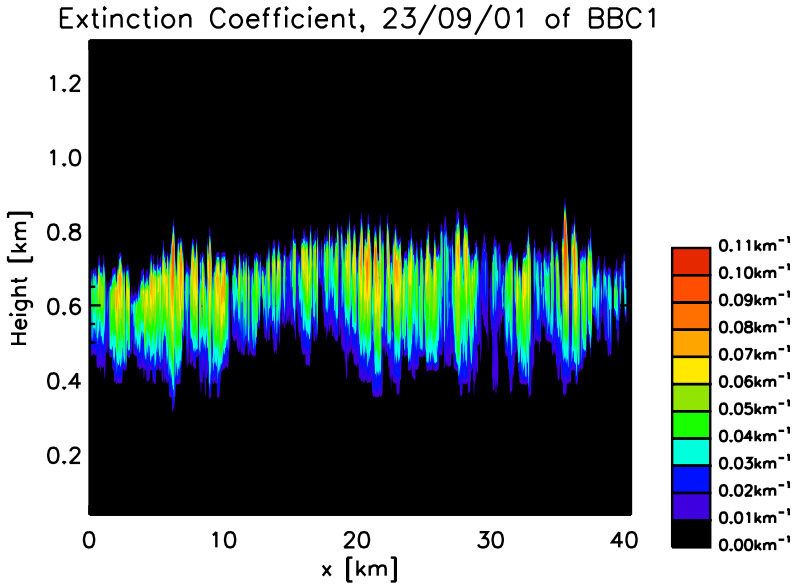

Figure 3: Extinction coefficient field corresponding to the LWC time series between 8:30 and 10:00h retrieved on September 23rd, 2001 of the BBC1 measurement campaign (see Fig. 2). This field was reconstructed by means of the Slingo parameterization, whereby a constant r_{eff} of 10 μm over the whole cloud field was assumed.

setup and the numerical conditions explained in Section 2 RT simulations for 5 nm-wide spectral bands covering the SWSR from 350 nm to 850 nm were performed by means of the LMCM. The solar zenith angle (SZA) was set to 50° (average value of the SZA for the time interval between 8:30 and 10:00 in the year's day 09/23/2001 and at Cabauw's latitude). A total of 10^7 photons was used for each spectral realization.

Figure 4 shows the transmission (T), the reflection (R), the absorption (A) and the apparent absorption (A_{app}) —the absorption that would be derived from in situ measurements of net vertical flux densities at two atmospheric levels— as a function of the wavelength. The energy balance is done for the whole atmosphere, i.e. T is computed at Earth's surface, R is computed at the top of the virtual atmosphere (TOA), A is the absorption within the whole atmosphere and A_{app} is the net vertical flux density difference at ground and at TOA. All these radiation fields are normalized to the downwelling irradiance at the top of the virtual atmosphere.

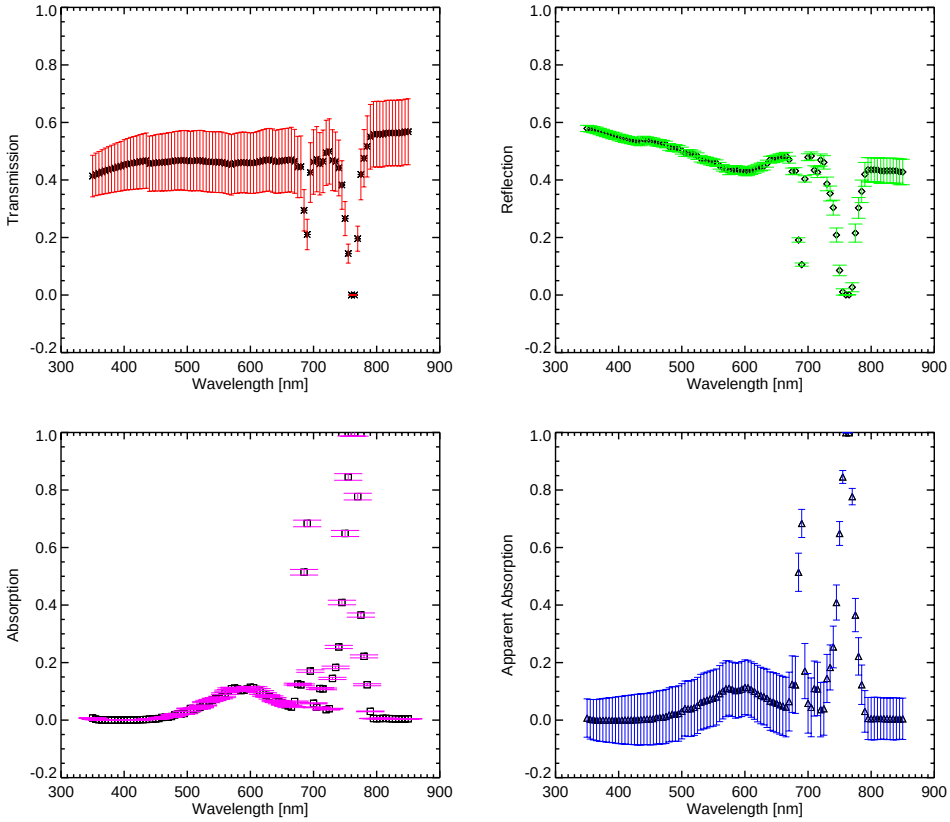

Figure 4: Domain-averaged spectral radiative quantities for the extinction coefficient field retrieved for the day of September 23rd, 2001 of the BBC1 measurement campaign (see Fig. 3). Top Left: transmission, top right: reflection, bottom left: absorption, bottom right: apparent absorption. The vertical bars represent horizontal spatial variability.

Each point in the plots of the figure 4 represents the mean value of the spectral radiative quantities, $\bar{Q}$, horizontally averaged over the whole region,

$$\bar{Q} = \frac{1}{N}\sum_{i=1}^{N} Q_i \,, \tag{8}$$

where Q represents all the radiative quantities ($Q = T, R, A, A_{\mathrm{app}}$) presented in figure 4, the subscript i goes through all the horizontal cells and N is the total number of horizotal cells. Additionally, each point of the plots has associated an "error bar" that represents the standard deviation of the mean value of spectral radiative quantities, $\mathcal{E}\left(\bar{Q}\right)$, over the whole domain,

$$\mathcal{E}\left(\bar{Q}\right) = \sqrt{\frac{1}{N}\sum_{i=1}^{N}\left(Q_i - \bar{Q}\right)^2} \,. \tag{9}$$

The standard deviation gathers information about the variability of the fields. The number of photons used in the MC realizations guarantees the contribution of the computational error to this variability to be negligible. All atmospheric components except clouds are horizontally homogeneous. Thus, the only explanation for the high variability of the T-field is the effect of the cloud inhomogeneities. The variability on R-field is much smaller since it is computed at TOA and the cloud inhomogeneities effects have been

smoothed out at this altitude. The A-field is much less sensitive to cloud inhomogeneities since liquid water is a weak absorber in the SWSR and because the nature of the absorption process is not photon incoming direction dependent. The mean value of A_{app} meets the mean value of A for all spectral bands. However, A_{app} shows much greater variability. Two main reasons are behind this variability: a) because A_{app} has indeed the contributions of the net horizontal flux (H) from one column to its neighbors and H-field is highly dependent on cloud inhomogeneities, and b) because of the variability of the upwelling and downwelling irradiances, since A_{app} is computed as a net vertical flux difference. The ozone's Chappuis Band in the visible region between 380 nm and 750 nm can be easily identified. More prominent are the oxygen A-Band (centered at 760 nm) and B-Band (centered at 688 nm).

These results should be compared with airborne radiation measurements. Unfortunately, the weather conditions did not allow simultaneous in situ measurements of the downward and upward flux densities on September 23rd, 2001 and consequently the RT model results can not be validated with the measurements from this particular day.

5.2 Radiative transfer for a LES-simulated Cumulus field and one IAAFT-surrogate

Figure 5 shows the extinction fields of a LES-simulated cloud (template) and an IAAFT-generated cloud with the same amplitude distribution and power spectrum (surrogate). Making use of the Slingo parameterization (Eq. 5), the proportionality of r_{eff} to r_v (Eq. 6) and the linear relationship $\gamma(N_c)$ found by Peng and Lohmann (2003) (Eq. 7), and considering a cloud number concentration of 1000 droplets/cm^3, the LWC was transformed into the 3D optical fields $\beta_{ext}(x,y,z)$, $\omega_0(x,y,z)$ and $g(x,y,z)$.

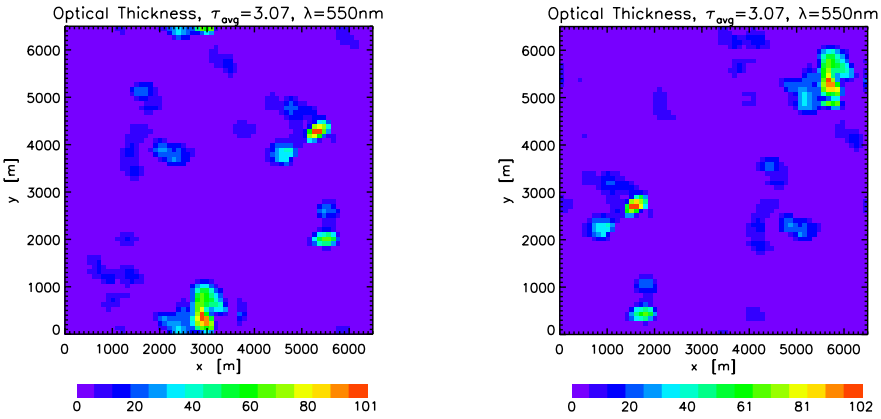

Figure 5: a) Optical thickness of a cumulus cloud LES-generated from measured data within the ARM (=**A**tmospheric **R**adiation **M**easurement) program (ARM (2004)). b) Optical thickness of an IAFFT-generated cloud, i.e. the surrogate cloud, with the same statistics as the cloud field in a).

Using the atmospheric setup and the numerical conditions explained in Section 2 RT simulations for a wavelength of 550 nm were performed by means of the LMCM. The SZA was set to 60°. A total of 10^8 photons for each spectral realization was used. Figure 6 shows top down the T-fields calculated at ground, the R-fields calculated at TOA, the A-fields within the whole atmosphere and the H-fields between the atmospheric columns for both, the template (left side) and the surrogate clouds (right side).

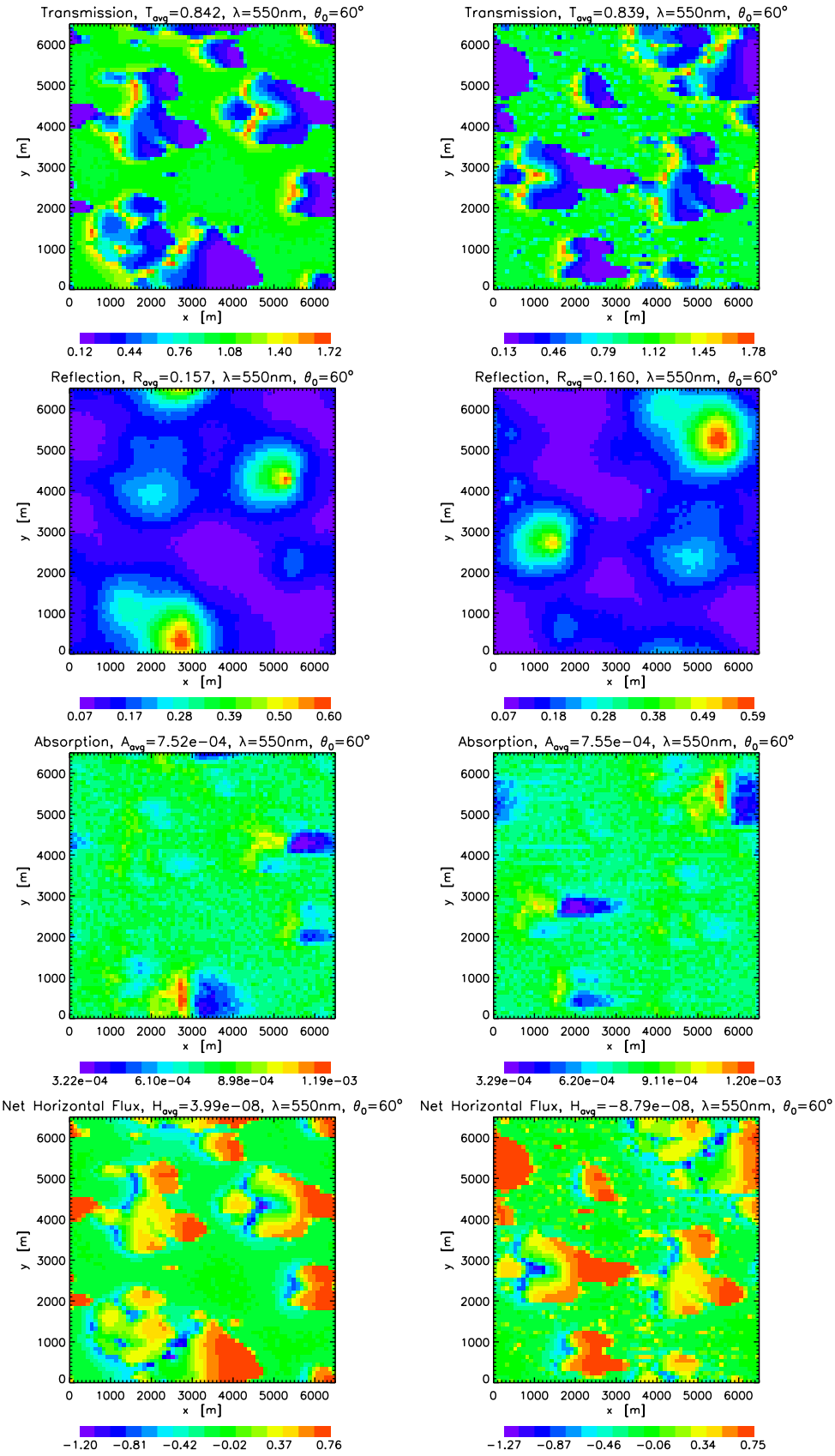

Figure 6: Left column: Transmission, Reflection, Absorption and Net Horizontal Flux fields for a LES-generated cumulus cloud from measured data within the ARM program. Right column: Transmission, Reflection, Absorption and Net Horizontal Flux fields for a IAAFT-generated surrogate cloud with the same statistics as the original cloud field.

T-fields show the shadows that the cumulus clusters lead into the solar light direction. An enhancement of T can be noticed at the pixels where the extra photons reflected at cloud edges end up. R-fields show high intensity pixels where the direct light comes reflected from dense cumulus nucleus. A-fields are very small since atmospheric constituents absorb weakly at this wavelength. Liquid water does not absorb at all for this wavelength. Nevertheless, multi-scattering within clouds increase the photon path length and thereby the probability of a photon to be absorbed by the atmospheric gases in this region. The study of H is of special interest as it is negligible in most of retrieval algorithm and dynamical models and therefore one of the main sources of errors. It can be noticed that H is comparable to T and R (if not bigger) in highly inhomogeneous regions when direct light arrives from high zenith angles. A mean value of H of zero does not necessarily mean that in reality H averages out in the whole domain since it is a direct consequence of the periodic boundary conditions.

Both, the template and surrogate cloud have the same amount of liquid water. Although they differ in spatial distribution they have nearly the same fractal structure. These characteristics seem to be enough to parameterize the cloud in terms of radiative properties as they lead to the same mean values of T and R averaged over the whole domain.

6 Conclusions and outlook

Cloud inhomogeneities in LWC have a strong influence on the radiative fields. Also estimation of cloud absorption via net vertical flux difference above and below the cloud are subjected to big bias coming from the neglect of the horizontal transport and from the variability of the flux densities themselves.

The same spectral radiative study presented here will be carried out in the future for other measured cloud fields and the results validated with airborne in situ measurements.

The climate and weather forecasting communities are claiming for a better parameterization of cloud radiative properties. The employment of surrogate clouds with predefined cloud statistics will surely speed up this find, as systematic studies can be easily scheduled.

Acknowledgments

This research project is funded by the Bundesministerium für Bildung und Forschung (BMBF) within the research programme AFO2000. We would like to thank V. Venema, U. Löhnert, M. Wendisch and J. Meywerk for the data provided. We would like to thank also the other members of the 4DCLOUDS project and the rest of participants on the BBC1 and BBC2 campaigns for the availability of the data on the BBC1 on BBC2 data bases.

Addresses of the Authors:

Sebastián Gimeno García, Institut für Meteorologie, Universität Leipzig, Stephanstr.3, 04103 Leipzig.

PD Dr. Thomas Trautmann, Institut für Methodik der Fernerkundung, Deutsches Zentrum für Luft- und Raumfahrt e.V. (DLR), Oberpfaffenhofen, 82234 Wessling

References

4DCLOUDS (2004). 4DCLOUDS project homepage. http://www.meteo.uni-bonn.de/projekte/4d-clouds/index.html; accessed February 1, 2004.

ARM (2004). Homepage of the Atmospheric Radiation Measurement program. http://www.arm.gov/; accessed February 1, 2004.

BBC1 (2004). Homepage of the Baltex Bridge Cloud campaign. http://www.knmi.nl/samenw/cliwa-net/setup/bbc/; accessed February 1, 2004.

BBC2 (2004). Homepage of the second Baltex Bridge Cloud campaign. http://www.knmi.nl/samenw/bbc2/main.html; accessed February 1, 2004.

CESAR (2004). Homepage of the Cabauw Experimental Site Atmospheric Research Working Groups. http://www.knmi.nl/samenw/cesar/; accessed February 1, 2004.

CLIWA-NET (2004). Homepage of the Cloud Liquid Water Network. http://www.knmi.nl/samenw/cliwa-net/; accessed February 1, 2004.

Crewell, S., Czekala, H., Löhnert, U., Rose, T., Simmer, C., and Zimmermann, R. (2001). Microwave radiometer for cloud cartography: A 22-channel ground-based microwave radiometer for atmospheric research. *Radio Sci.*, **36**, 621–638.

Deardorff, J. W. (1972). Numerical investigation of neutral and unstable planetary boundary layers. *J. Atmos. Sci.*, **29**, 91–115.

Frisch, A. S., Fairall, C. W., Feingold, G., Utal, T., and Snider, J. B. (1998). On cloud radar and microwave radiometer measurements of stratus cloud liquid water profiles. *J. Geophys. Res.*, **103**(23), 195–197.

GESIMA (2004). Homepage of the Geesthacht Simulation Model of the Atmosphere. http://w3g.gkss.de/staff/kapitza/gesima/; accessed February 1, 2004.

Gimeno, S. and Trautmann, T. (2003). Radiative transfer modeling in inhomogeneous clouds by means of the Monte Carlo method. *Wiss. Mitt. LIM*, **30**, 29–43.

KNMI (2004). Homepage of the Koninklijk Nederlands Meteorologisch Instituut. http://www.knmi.nl/; accessed February 1, 2004.

Löhnert, U., Crewell, S., and Simmer, C. (2003). An integrated approach towards retrieving physically consistent profiles of temperature, humidity and cloud liquid water. *Submitted to J. Appl. Meteor.*.

LM (2004). Homepage vom Lokal Model, Deutscher Wetterdienst (DWD). http://www.dwd.de/de/FundE/Analyse/Modellierung/lm.htm; accessed February 1, 2004.

McClatchey, R. A., Fenn, R. W., Selby, J. E. A., Volz, F. E., and Garing, J. S. (1972). Optical properties of the atmosphere. AFCRL 0497, Air Force Cambridge Research Laboratories.

MIRACLE (2004). Homepage of the 95 GHz polarimetric cloud doppler radar MIRACLE. http://w3.gkss.de/english/Radar/miracle.html; accessed February 1, 2004.

Peng, Y. and Lohmann, U. (2003). Sensitivity study of the spectral dispersion of the cloud droplet size distribution on the indirect aerosol effect. *Geophys. Res. Lett.*. 10.1029/2003GL017192.

Rothman, L. S. *et al.* (1998). The HITRAN molecular spectroscopic database and HAWKS (HITRAN atmospheric workstations): 1996 edition. *Quant. Spectrosc. Radiat. Transfer*, **60**, 665–710.

Scheirer, R. and Macke, A. (2001). On the accuracy of the independent column approximation in calculating the downward fluxes in the UVA, UVB, and PAR spectral ranges. *J. Geophys. Res. Atmos.*, **106**(D13), 14301–14312.

Slingo, A. (1989). A GCM parameterization for the shortwave radiative properties of water clouds. *J. Atmos. Sci.*, **46**, 1419–1427.

Stamnes, K., Tsay, S.-C., Wiscombe, W., and Jayaweera, K. (1988). Numerically stable algorithm for discrete-ordinate-method radiative transfer in multiple scattering and emitting layer ed media. *Appl. Opt.*, **27**, 2502–2509.

Venema, V., Meyer, S., Gimeno G., S., Simmer, C., Crewell, S., Löhnert, U., Trautmann, T., and Macke, A. (2003). Iterative Amplitude Adapted Fourier Transform surrogate cloud fields. *Submitted to JGR*.

Wendisch, M., Pilewskie, P., Jäkel, E., Schmidt, S., Pommier, J., Howard, S., Jonsson, H. H., Guan, H., and Schröder, M. (2003). Airborne measurements of areal spectral surface albedo over different sea and land surfaces. *Submitted to J. Geophys. Res.*.